

Grain boundary separation in transgranular cleavage cracking

J. Chen¹, X. Kong², S. S. Chakravarthula² and Y. Qiao*¹

The energy balance associated with the transmission of cleavage front across high angle grain boundary is analysed theoretically. On the one hand, if the distance between adjacent break-through points is small, their crack trapping effect tends to be pronounced. On the other hand, decreasing this distance promotes the separation of persistent grain boundary areas. The effective grain boundary toughness is also dependent on the profiles of penetrating front sections and the surface free energy of grain boundary. The most energetically favourable crack front transmission mode can be reached through a self-adjusting process.

Keywords: Cleavage cracking, Grain boundary, Fracture toughness, Break-through point

Introduction

In the framework of classic linear elastic fracture mechanics (LEFM), it is assumed that the fracture initiation of a brittle material is triggered by pre-existing microcracks.¹ The microcracks are often grain sized, i.e. their fronts are arrested by surrounding grains. They are usually formed due to internal stresses associated with processing and post-processing treatments as well as handling and machining.² When the material is subjected to a high external loading, the microcracks of favourable orientations can overcome the barrier of grain boundaries. As the crack propagation becomes unstable, catastrophic failure would occur. Under this condition, the fracture toughness of an un-notched brittle material is dominated by the resistance offered by grain boundaries to cleavage cracking.

Recently, the grain boundary toughness was investigated experimentally by Qiao and Argon in considerable detail.^{3–5} As a cleavage front is arrested by a high angle grain boundary where the twist and tilt angles are larger than about 10°, with an increasing stress intensity, the front would penetrate across the boundary at a number of break-through points (BTPs), leaving the grain boundary behind the verge of propagating front at persistent grain boundary islands (PGBI). Owing to the crystallographic misorientations and the crack front branching, after the front enters the next grain it would advance in a set of parallel terraces, leading to the formation of well known river markings. Such crack boundary interactions have been observed repeatedly in many brittle materials, as can be seen in Fig. 1.⁶

Depending on the grain boundary strength and the break-through mode, the PGBI can act as either tough reinforcements, which bridge across fracture flanks even

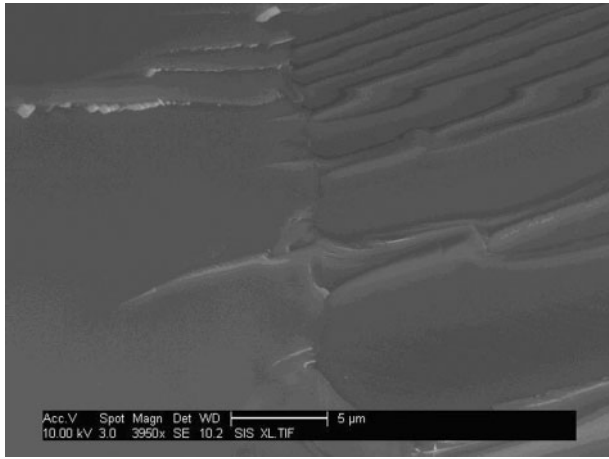
after their trapping effect is overcome,⁷ or debondable reinforcements, which are separated apart simultaneously as the crack front bypasses the boundary.^{5,8} In the former case, the grain boundary is not completely separated when the crack front penetrates through it. Rather, the crack would go a round about way to surround the PGBI, somewhat similar to the cracking process in a brittle matrix composite material reinforced by tough fibres.⁹ The cleavage crack must overcome the crack trapping effect of the PGBI, and once the two front parts at both sides of a PGBI merge into a new one, it can continue to advance in the next grain. In the latter case, the barrier effect of boundary is caused by the additional fracture work required to shear apart the PGBI. As the penetration depth of the front increases, since more and more grain boundary is involved in the front transmission, the overall fracture resistance rises, resulting in an *R* curve.¹⁰ As the increase rate of crack growth driven force is balanced by the increase rate of resistance, the crack growth becomes unstable and the grain boundary fails.

In the above discussion, it is assumed that the crack front transmission pattern is known. While the cleavage surfaces across a grain boundary are quite determinant if the crystallographic orientations of the two grains are given, a deep understanding of the factors that govern the distance between the BTPs is still lacking. A grain boundary can be regarded as a thin layer of highly disordered atoms.¹¹ If its shear strength is high enough, it can bear large bridging stresses as it is exposed to a crack front. The competition between the shearing of boundary and the river marking formation causes a relatively regular break-through mode.¹² However, in many brittle materials, such as silicon, the grain boundaries are relatively weak. They would separate before their crack trapping effect is fully overcome, and therefore, the crack front transmission should not be affected by the post-critical front advance. According to experimental measurements,^{3–5} the most probable BTP distance is around 2–3 μm. Since this range is much larger than the characteristic length scale of grain

¹Department of Structural Engineering, University of California at San Diego, La Jolla, CA 92093 0085, USA

²Department of Civil Engineering, University of Akron, Akron, OH 44325 3905, USA

*Corresponding author, email yqiao@ucsd.edu



1 Image (SEM) of cleavage cracking across high angle grain boundary in boron doped polycrystalline silicon: crack propagates from right to left

boundary structure, it must be determined by the crack tip stress field. Note that, nominally, the most energetically favourable BTP distance should be zero, not the measured value (2–3 μm), since when BTPs are near each other little additional grain boundary needs to be separated apart.

In the present paper, the authors analyse the grain boundary separation process as a cleavage front penetrates through it. The result shows that the grain boundary toughness is highly dependent on the distance between BTPs. As the crack front segments penetrate across the boundary, it is the rate of increase of grain boundary resistance, instead of the boundary resistance itself, which dominates the final failure criterion, leading to a self-optimised BTP distance close to the experimental data.

Distribution of local stress intensity along crack front

The crack front penetration process is schematically shown in Fig. 2a. The crack propagates from grain ‘A’ to ‘B’ through the grain boundary. It penetrates through the breakthrough points that distribute along the boundary periodically. The BTP distance is w . As the overall crack tip stress intensity rises, the penetration

depth increases, and once it reaches the critical value the persistent grain boundary islands between BTPs, which are shown as the shaded areas, are separated apart and thus the barrier effect of the boundary is overcome. Since the front enters into grain ‘B’ at different BTPs, due to the crystallographic misorientations the fracture surface in grain ‘B’ consists of a number of parallel terraces. The cleavage ridges, i.e. the secondary fracture facets, are known as river markings. However, they are formed after the boundary is fully overcome and therefore should not affect the critical condition of PGBI separation.

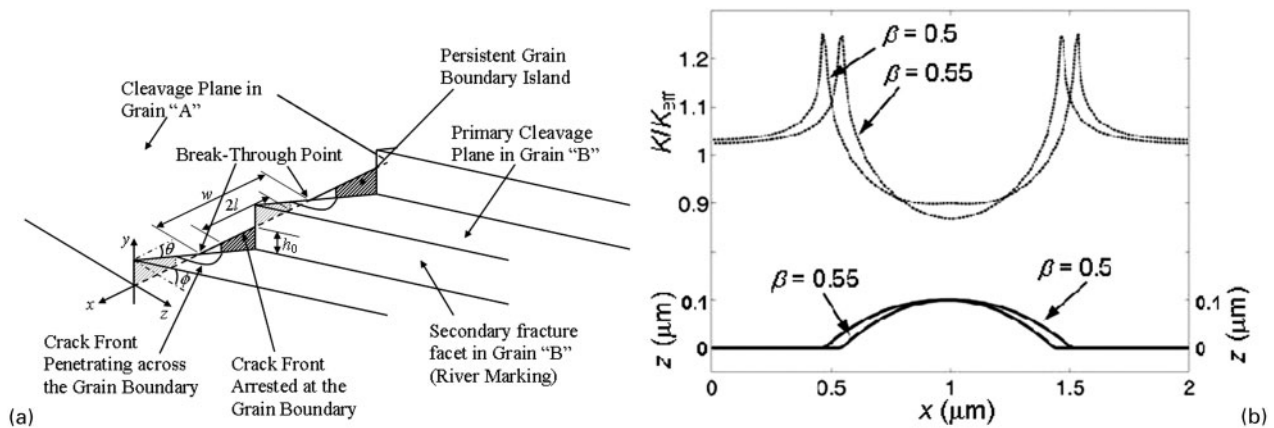
In order to analyse the crack front transmission mode, it is important to understand the local stress intensity distribution. As can be seen in Fig. 2b, when the crack front penetrates across the boundary, the local stress intensity factor can be calculated using a first order method¹³

$$K(x) = K_0[x; a(x)] + \frac{1}{2\pi} \int_{\Omega} \frac{K_0[\tilde{x}; a(x)][a(\tilde{x}) - a(x)]}{(\tilde{x} - x)^2} d\tilde{x} \quad (1)$$

where x is the axis along the grain boundary, $a(x)$ is the local crack length, $K_0[x; a(x)]$ is the reference stress intensity factor of a straight front with the crack length of $a(x)$, and Ω denotes the entire crack front. An ‘exact’ solution of equation (1) for the profile of the protruding front, $a(x)$, can be obtained numerically by setting $K(x)$ to be a constant K_B at the verge of propagating front.^{14,15} with K_B being the effective fracture toughness of grain ‘B’. The value of K_B can be assessed as $K_{cry}/(\cos\theta\cos\phi)^{1/2} \cos\theta\cos\phi$, where K_{cry} is the crystallographic toughness of the material, and θ and ϕ are the twist and tilt misorientation angles, respectively. At the level of first order approximation, for the sake of simplicity, a less computationally expensive way to solve equation (1) is to assume that¹⁰

$$\frac{z}{w} = \begin{cases} \frac{\Delta a}{w} - \left(\frac{|x-x_0|}{w}\right)^{1/\beta} & \text{when } |x-x_0| < w(\Delta a/w)^\beta \\ 0 & \text{elsewhere} \end{cases} \quad (2)$$

where $z(x)$ is the profile of the penetrating crack front segment in grain ‘B’; w is the distance between adjacent BTPs; Δa is the penetration depth, i.e. the distance from the tip of the protruding front to the grain boundary; x_0 is the location of the centre point of BTP; and β is a

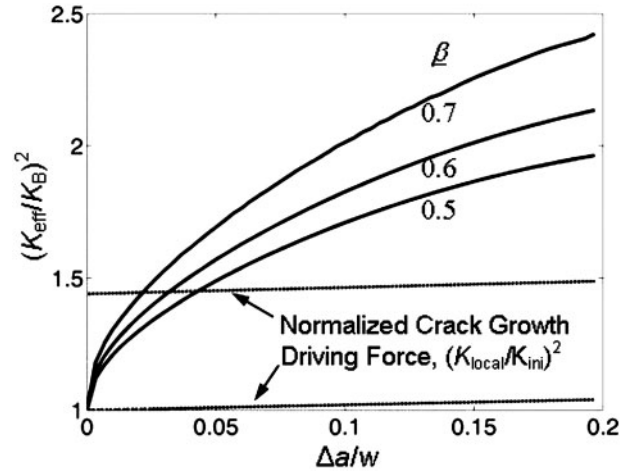


2 a Schematic diagram of cleavage crack propagating across high angle grain boundary (crack propagates from left to right) and b top view of crack propagates from bottom to top around BTP (solid lines indicate crack fronts and broken lines indicate local stress intensity)

parameter to be determined. By substituting equation (2) into equation (1), $K(x)$ can be calculated explicitly.

The broken lines in Fig. 2b show the distributions of local stress intensity, where K_{eff} is the reference stress intensity factor for a crack with a straight front at the boundary; w is taken as $2 \mu\text{m}$, and Δa is $0.05w$. Without losing generality, it was assumed that the crack was in a double cantilever beam specimen, and therefore with a constant remote loading the crack tip stress intensity factor was proportional to $1/a(x)^2$. The boundary was assumed to be infinitely wide. The integration zone in equation (1), Ω was taken as the part of crack front within $5w$ from the point under consideration, i.e. the influence of features of crack front more than $5w$ away was ignored. Increasing the integration range would not cause detectable variations in the numerical result of $K(x)$. It can be seen that at the protruding part of the crack front, the local stress intensity is smaller than K_{eff} , and that at the boundary is larger. That is, the front segments left behind (the concave parts) have a 'shielding effect' on the convex parts; the front motion would, otherwise, be unstable. If the material properties were homogeneous, with an initial perturbation on front profile, the growth of protruding front segments would be suppressed and the advance of the rest part would be accelerated, and as a result the front tends to be straight again. In the central part of a concave or a convex segment, the distribution of $K(x)$ is relatively uniform, while at the border $K(x)$ changes in a large range. In fact, the local stress intensity at the turn point of the crack front tends to infinity, since it is a sharp corner. When x moves away from the turn point, $K(x)$ rapidly decreases and forms a plateau. The transition zone at the border is of a complicated configuration. Since the cleavage plane must shift its orientation across the boundary, the structure of the border of front segments is three-dimensional, and therefore its behaviours cannot be captured by the simplified model of equation (1). According to experimental observations that river markings in grain 'B' around a BTP were quite smooth,³⁻⁵ the crack front penetration is governed by the advance of the entire convex part.¹⁰ Therefore, in the following discussion, the authors will focus on the value of $K(x)$ at the central part of each front segment.

If K_{eff} were constant, as long as $\Delta a/w$ and β do not change, $K(x)$ is independent of the values of w . However, since K_{eff} is a function of \tilde{x} , $K(x)$ is non-scalable. As w becomes larger, with a similar front profile, the influence of the term of $a(\tilde{x}) - a(x)$ in equation (1) is reduced and therefore the distribution of $K(x)$ is more uniform; that is, the stress intensity at the PGBI is smaller and at the penetrating front segment is larger. Moreover, when w rises, β is no longer a constant. As two PGBIs are far away from each other, the penetrating front segment in between tends to be wider and flatter, and thus the value of β is smaller, which is reflected by the fact that β must decrease as w increases so that the distribution of $K(x)$ at a BTP would remain nearly uniform. In a real specimen, as the crack stably penetrates into grain 'B', the local stress intensity along the front should be balanced by the local fracture toughness K_B . At the first order approximation level, it is difficult, and unnecessary, to keep the distribution of $K(x)$ uniform along boundary. In the



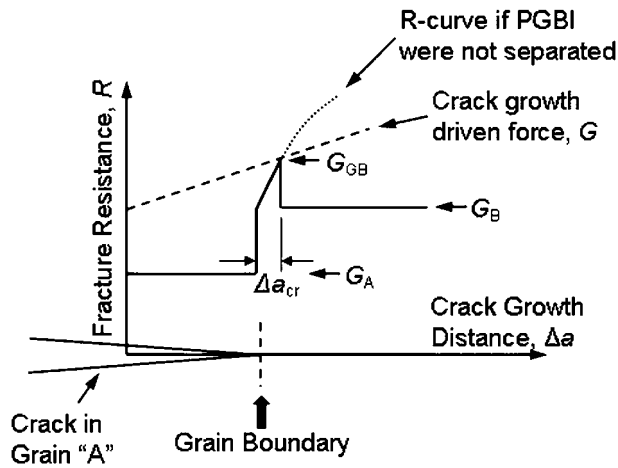
3 Fracture resistance as function of penetration depth
 Δa : local stress intensity at verge of propagating crack front is K_B ; broken lines indicate normalised crack growth driving forces, with initial crack length set to $10w$; upper broken line is for $K_{\text{ini}}=K_B$ when $\Delta a/w=0$; lower broken line is for $K_{\text{ini}}=1.2K_B$ when $\Delta a/w=0.032$, where K_{ini} is initial effective stress intensity factor

current study, β was determined as the optimum value that minimised the aspect ratio of the $K(x)$ distribution curve in the central part of penetrating front segment to <0.1 . The variation in $K(x)$ along the boundary does not significantly affect the following calculation since the failure criterion is determined by the central part. For a large w , β was ~ 0.5 , and as w decreased, β increased to nearly 0.7 .¹⁰ In the range of w of 0.5 to $10 \mu\text{m}$, the numerical results can be regressed as $\beta = 0.51 + 0.09/\tilde{w}$, where $\tilde{w} = w/w_0$ and $w_0 = 1 \mu\text{m}$ is the characteristic BTP distance. Figure 2b shows that, as β increases, i.e. when the protruding front segment is 'sharper', the degrees of increase in $K(x)$ in concave front segment and decrease in convex front segment are larger, and thus to maintain K_B at the protruding front, the nominal applied stress intensity factor, K_{eff} , must also increase.

Penetration of crack front across grain boundary

Initially, when the crack front is entirely arrested by the grain boundary, it is straight and the distribution of $K(x)$ is uniform. As the crack tip stress intensity factor reaches K_B , the front starts to penetrate across the boundary at a number of BTPs, with the rest of it being arrested by PGBI. If the applied loading did not increase, since the local stress intensity at the tip of protruding front segment would decrease, the front transmission would immediately stop. As the applied load rises, the penetration depth would increase accordingly, with the local stress intensity at the protruding front being K_B , as can be seen in Fig. 3. With a constant β , K_{eff} increases rapidly as Δa becomes larger. With a variation of $\Delta a/w$ of only 0.1 , $(K_{\text{eff}}/K_B)^2$ increases by nearly 75% , forming a steep resistance R curve. As β increases, the R curve is even steeper since, with a constant Δa , the required K_{eff} is higher.

The crack front would advance stably if this process continues. There are several possible mechanisms to trigger the unstable crack propagation and the final failure of the grain boundary. In the framework of the



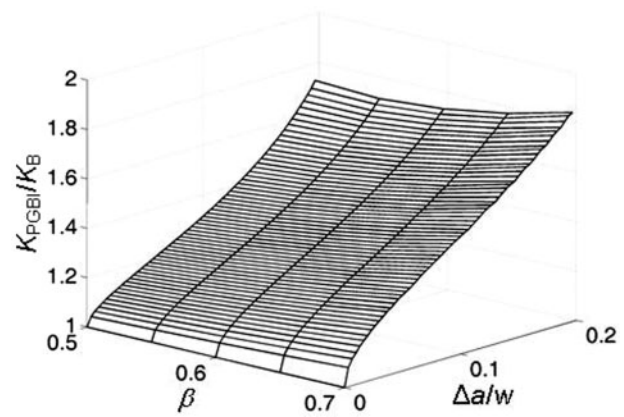
4 Schematic diagram of R curve analysis

classic R curve analysis,¹⁰ the crack growth is stable when the crack growth driving force G , equals to the fracture resistance R , while $dG/da < dR/da$. That is, while both G and R increase with crack length, the rate of increase of G is smaller. Therefore, when $G=R$ the crack grows, but with an incremental crack growth R would exceed G , and thus the crack stops. Only when dG/da is equal to or larger than dR/da , can the crack growth become unstable. The solid lines in Fig. 3 indicate the R curves, and the broken lines indicate G , which was taken as $(K_{local}/K_{ini})^2$, where K_{ini} is the initial stress intensity factor when the crack front is arrested at the boundary, and K_{local} is the stress intensity factor when the penetration depth is Δa . It can be seen that while both R and G are increasing curves, the increase rate of R is much higher. Hence, in the ranges of parameters under consideration, the critical condition of $dG/da = dR/da$ can never be reached.

Grain boundary separation and grain boundary toughness

As the penetration depth of the crack front keeps increasing, the width of the breakthrough window would be wider and wider. However, even when the break-through window width rises to w , i.e. in the top view the protruding front segments start to overlap with each other, as long as the PGBI still bridge across the fracture flanks, the grain boundary would still suppress the crack front advance. Under this condition, owing to the complicated undercutting and bending of cleavage terraces (the primary cleavage planes) in grain 'B', a process zone would be formed behind the crack front, and the overall grain boundary fracture resistance is dominated by the competition of crack trapping effect and bridging effect.¹² To minimise the crack trapping effect of grain boundary, the BTP distance should be zero, so that no grain boundary would be involved, which is inconsistent with the result of fractography study.³⁻⁵

Clearly, the PGBI separation plays a critical role in the crack front transmission process. As depicted in Fig. 4, initially when the crack front is in the first grain ('A'), the local fracture resistance is G_A , the crystallographic resistance of grain 'A'. As the front reaches the grain boundary, the crack growth driven force must be increased to G_B so that the front can start to



5 Local stress intensity at persistence grain boundary island K_{PGBI} as function of penetration depth and crack front profile

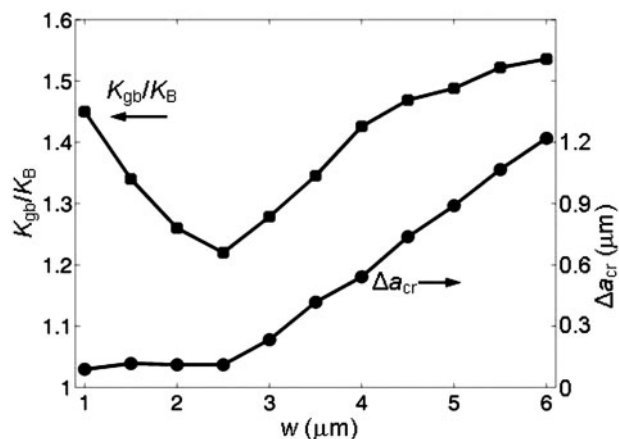
penetrate into the next grain ('B'), where G_B is the crystallographic resistance of grain 'B'. As G keeps increasing, the penetration depth would become increasingly large. If the PGBI were perfect, R would increase monotonically, as shown by the dotted line, and therefore dR/da is always larger than dG/da . If, on the other hand, with the increase in local stress intensity at the front segment arrested at the boundary, K_{PGBI} , the PGBI is separated apart, because the abrupt decrease in R to G_B , both requirements that $G > R$ and $dG/da > dR/da$ are satisfied, and consequently the crack growth becomes unstable.

The PGBI separation can be regarded as a mode II fracture along the boundary.¹⁶ The critical condition can be stated as $\tau|_{y=y_0} = \tau_{gb}$, where τ is the crack tip shear stress, y indicates the axis normal to the cleavage plane, y_0 is a critical distance and τ_{gb} is the effective shear strength of grain boundary, which was experimentally determined as 144 MPa.⁴ If the failure criterion of the grain boundary is that the entire PGBI yields, y_0 should be taken as the height of PGBI, $h_0 = (w/2) \tan \theta$. Hence, the critical local stress intensity factor at PGBI can be written as

$$K_{PGBI}^{(cr)} = \alpha \tau_{gb} (\pi w \tan \theta)^{1/2} \tag{3}$$

where α is a geometry factor. If it is assumed that the grain boundary is normal to the cleavage plane in grain 'A', $\alpha = 0.3531$.¹⁷ It can be seen that $K_{PGBI}^{(cr)}$ increases linearly with $w^{1/2}$ and $(\tan \theta)^{1/2}$.

The increase in K_{PGBI} with the crack front penetration depth can be seen in Fig. 5. As expected, the overall stress intensity factor must be raised to drive the crack front advance in grain 'B', so is the local stress intensity factor at PGBI. The value of K_{PGBI} is also dependent on β . On the one hand, as β increases the penetrating front segment becomes narrower and sharper, and the increase in local stress intensity at PGBI is less pronounced; consequently, K_{PGBI} tends to decrease. On the other hand, the 'shielding effect' of PGBI increases with β ; that is, the local stress intensity at the protruding front segment decreases, and therefore to keep the front from stopping a higher overall stress intensity factor must be applied, which tends to raise K_{PGBI} . As a result of the competition of the two mechanisms, with a given front penetration depth the $K_{PGBI}-\beta$ relationship can be non-monotonic. When the front penetration depth is



6 Grain boundary toughness K_{gb} and critical penetration depth Δa_{cr} as functions of distance between BTPs: value of β is taken as 0.6

relatively small, the latter mechanism is dominant and thus $dK_{PGBI}/d\beta$ is positive. When the front penetration depth is relatively large, at the smaller β range the former mechanism is more significant and $dK_{PGBI}/d\beta$ is negative, while at the larger β range an opposite relationship is observed. Note that the critical penetration depth is dependent on β . Hence, the constant $\Delta a/w$ lines do not represent the critical conditions of PGBI separation.

The grain boundary toughness K_{gb} , can be taken as the critical overall stress intensity factor K_{eff} , at which the two criteria of $K_{front} = K_B$ and $K_{PGBI} = K_{PGBI}^{(cr)}$ are satisfied simultaneously, where K_{front} is the local stress intensity at the protruding front segment. The front penetration depth corresponding to the critical condition is Δa_{cr} . As can be seen in Fig. 6, where the twist angle is set to 22.5° , the mean of random orientation, both of K_{gb} and Δa_{cr} are functions of w . As w increases, since the profile of penetrating front segment becomes flatter, with the same K_{eff} the local stress intensity at the concave front segment is larger, and thus K_{gb} , tends to be smaller. However, according to equation (3), $K_{PGBI}^{(cr)}$ also increases with w , which would lead to a higher K_{gb} . If BTPs are close to each other, the front profile effect is pronounced, and therefore K_{gb} decreases as w increases. When BTPs are relatively far away from each other, the front profile variation is somewhat saturated, while h_0 becomes large, and thus $K_{gb}-w$ is a rising curve. There exists a critical BTP distance around $2.5 \mu m$, at which the grain boundary toughness is minimum. That is, as w equals to this optimum value, it is most energetically favourable for the crack front to overcome the barrier effect of the grain boundary.

If initially the BTP distance is larger, with the increase in applied loading, more and more BTPs will be activated, so that K_{gb} decreases. When the increasing K_{eff} reaches the decreasing K_{gb} , the grain boundary fails. If initially the BTP distance is smaller, some of the BTPs would be deactivated due to the 'shielding effect' of adjacent BTPs, and thus the effective w rises; again, once the increasing K_{eff} equals to the decreasing K_{gb} , the boundary is separated apart and the crack front transition process is completed. The self-adjustment of w has been observed in experiments, where the modal values of BTP distance distribution curves were always $2-3 \mu m$, quite independent of the grain orientations.⁴

The dependence on w of the normalised critical penetration depth $\Delta a_{cr}/w$, is similar to that of K_{gb} .

As w is smaller than the critical value, $\Delta a_{cr}/w$ decreases as the BTP distance increases; and as w is larger, the relationship is opposite. However, the $\Delta a_{cr}-w$ relation is monotonic. When w is relatively large, $d\Delta a_{cr}/dw$ is nearly constant, which should be attributed to the combined effect of β variation and $K_{PGBI}^{(cr)}$ increase. Note that the above analysis is based on the assumption that the crack growth distance is much smaller than the initial crack length; otherwise not only the reference stress intensity factor calculation is no longer relevant, but also the periodic distribution of BTPs along grain boundary (Fig. 2) becomes impossible. For w around $2-3 \mu m$, the precrack size should be larger than $10 \mu m$. For shorter precracks, unless w is significantly lowered, this model should not be applied.

Conclusions

The grain boundary separation condition in transgranular cleavage cracking is investigated. For a high angle grain boundary which can be separated apart during the crack front transmission process, the factors that govern the distance between BTPs are analysed. The current investigation is in the context of LEFM and only for quasi-static fracture of 'purely' brittle materials. If crack-tip blunting or dynamics effects are pronounced, the model must be modified, e.g. by using effective material parameters, to reflect the variations in crack tip stress field. Nevertheless, through our discussion, it is demonstrated that as the crack front penetrates through the grain boundary the persistent grain boundary islands are subjected to increasingly high local stress intensity. When it reaches a critical value, the grain boundary fails and its barrier effect is overcome. As the BTP distance increases, larger grain boundary area needs to be separated apart and thus the grain boundary toughness tends to increase. As the BTP distance is small, on the other hand, with an increasing crack front penetration depth, since the rate of increase of fracture resistance is lower, it is more difficult to reach the critical condition of unstable crack advance and thus the effective boundary toughness also tends to rise. The competition of the two mechanisms leads to an optimum BTP distance. The following conclusions are drawn.

1. The grain boundary toughness is highly dependent on the distance between BTPs. There exists a critical distance at which the grain boundary toughness is minimised. Under this condition, it is most energetically favourable for the crack front to bypass the boundary.
2. The grain boundary toughness is also determined by the profile of crack front and the critical condition of grain boundary separation.
3. The critical crack front penetration depth increases monotonically with the distance between BTPs. However, the normalised critical depth has a similar BTP distance dependence with the grain boundary toughness.
4. Through self-adjusting, the crack front penetrates across the boundary with the BTP distance close to the critical value.

Acknowledgements

This work was supported by The Office of Basic Energy Science, The Department of Energy under grant

no. DE-FG02-05ER46195. Special thanks are also due to Professor K. J. Hsia and Professor E. Pan for the useful discussions and valuable suggestions.

References

1. T. L. Anderson: 'Fracture mechanics: fundamentals and applications'; 2004, Boca Raton, FL, CRC Press.
2. R. J. Sanford: 'Principles of fracture mechanics'; 2002, Englewood Cliffs, NJ, Prentice Hall.
3. A. S. Argon and Y. Qiao: *Philos. Mag. A*, 2002, **82A**, 3333–3348.
4. Y. Qiao and A. S. Argon: *Mech. Mater.*, 2003, **35**, 129–154.
5. Y. Qiao and A. S. Argon: *Mech. Mater.*, 2003, **35**, 313–331.
6. Y. Qiao and X. Kong: *Met. Mater. Int.*, 2006, **12**, 27–30.
7. X. Kong and Y. Qiao: *Fatig. Fract. Eng. Mater. Struct.*, 2005, **28**, 753–758.
8. Y. Qiao and X. Kong: *Mater. Lett.*, 2004, **58**, 3156–3160.
9. T. M. Mower and A. S. Argon: *Mech. Mater.*, 1995, **19**, 343–364.
10. Y. Qiao: *Mater. Sci. Eng. A*, 2003, **A361**, 350–357.
11. P. E. J. Flewitt and R. K. Wild: 'Grain boundaries: their microstructures and chemistry'; 2001, New York, John Wiley & Sons.
12. Y. Qiao, J. Chen, X. Kong and S. S. Chakravarthula: *Comput. Mater. Sci.*, to be published.
13. J. R. Rice: *J. Appl. Mech.*, 1985, **52**, 571–579.
14. A. F. Bower and M. Ortiz: *Trans. ASME*, 1993, **115**, 228–236.
15. A. F. Bower and M. Ortiz: *J. Mech. Phys. Solids*, 1991, **39**, 815–858.
16. F. A. McClintock: Proc. George Irwin Symp. on 'Cleavage fracture', (ed. K. S. Chan), 81; 1992, Warrendale, PA, TMS.
17. R. W. Hertzberg: 'Deformation and fracture mechanics of engineering materials'; 1989, New York, John Wiley & Sons.